6-1 (Invited)

Multiscale Simulation of Diffusion, Deactivation, and Segregation of Dopants – Ab-Initio to Continuum

Wolfgang Windl
Department of Materials Science and Engineering, The Ohio State University
2041 College Road, Columbus, OH 43210-1178, U.S.A.
E-mail: windl@mailaps.org

Abstract – **In this paper, concepts and applications of *ab-initio* based multiscale process simulation work are discussed, including results for diffusion, deactivation, and interface segregation of boron in silicon as well as a corresponding continuum model.**

I. INTRODUCTION

The silicon-based metal oxide semiconductor field effect transistor (MOSFET) is at the heart of today's semiconductor industry. Since the switching speed of MOSFETs increases linearly with shrinking dimensions, which, in turn, also allows for the packing of more MOSFETs on a chip of a given area, the semiconductor industry has managed to constantly improve the performance of computers by continuously scaling a more or less unchanged device geometry. This improvement follows closely Moore's law, which predicts performance doubling approximately every 18 months.

Despite the very successful history of device miniaturization in the past, the scaling age is currently reaching the physical limits of the traditional device materials. Hence, simulation of front-end processing becomes a more and more critical cost and especially time saving component of integrated-circuit technology development, provided it is accurate enough. In addition, today's electronics are so small that characterization of their material parameters is often very difficult and expensive. Simulation is in many cases the only effective tool for exploring the lateral and vertical doping profiles of a modern device at the level of detail required for optimization.

Increasingly, process simulation is being performed by "multiscale modeling", using a hierarchy of tools. *Ab initio* and molecular-dynamics (MD) codes are used to generate insight into the physics of mobility and reactions of atoms in the silicon lattice. This information can then be fed into higher-level modeling like Kinetic Lattice Monte Carlo codes (to establish the dominant, critical mechanisms, where they are not obvious) and traditional continuum codes which are used for production runs. In the following, some examples of recent research for B diffusion, deactivation, and segregation will be discussed.

II. BORON DIFFUSION IN SILICON

Boron diffuses nearly exclusively with the help of Si self-interstitials (*I*s),[1] i.e., the mobile entity is thought to be a B atom paired with an *I*. As concerning the diffusion mechanism, *ab-initio* modeling had suggested a few years ago that a kick-out mechanism with long-range low-barrier interstitial migration would be the dominant mechanism,[2] in contrast to previous perception. In that work, diffusion saddle point configurations had been guessed or estimated by dragging an atom "by hand" from minimum to minimum across the saddle.[2] However, such methods are often not reliable, especially if the diffusion involves the concerted motion of more than one atom.[3] Therefore, as described in Ref. 5, we used the nudged elastic band method (NEBM)[3] implemented into VASP[4] to re-examine the minimum-energy barrier diffusion path for *I*-assisted, charge-state dependent B diffusion.

The pair with the lowest formation energy that we found in the neutral case, BT^0 [Fig. 1(c); *T* denotes a tetrahedral self-interstitial], has a formation energy of 2.8 (2.5) eV + E_F with respect to the lowest-energy B charge state, B^-, with a binding energy of 0.9 (0.6) eV relative to the most stable dissociation products I^+ and B^- [here and in the following, numbers without (with) brackets denote GGA (LDA) results]. This contradicts previous work[2] which identified the configuration from Fig. 1(a) as the starting point for migration. Our binding energy is very similar to the sheer Coulomb attraction of a positive and a negative point charge (~0.6 eV). For the +1 charged system, the same configuration, BT^+, has the lowest formation energy with a binding energy of 1.0 (0.8) eV with respect to the dissociation products B^- and T^{++}. For the –1 charged system, we find two dumbbell-like interstitials with [110] and [100] orientation to have the lowest formation energies, B_X^- [Fig. 1(e)] and B_S^- [Fig. 1(f)], respectively. B_X^- has the lowest total energy with a binding energy of 0.5 (0.3) eV with respect to B^- and X^0.

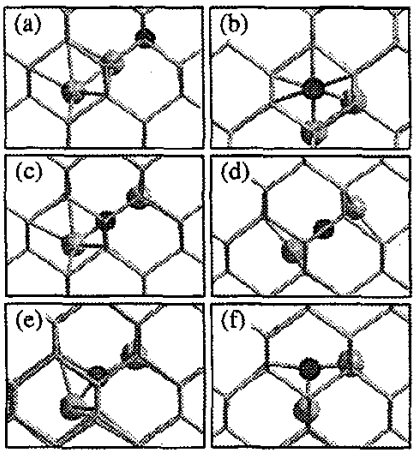

FIG. 1 B (black ball)-*I* pairs in Si (grey balls & sticks).

In contrast to the previously proposed B diffusion mechanism,[2] we find B_S and not B_T to play the central role in diffusion (even though it is not stable in the neutral charge state). In the neutral case, we find the BT^0 pair to migrate via the B_S^0 [Fig. 1(f)] to an B_H^0 [Fig. 1(b)] interstitial by a buckling of the Si-B-*T* triple dumbbell with a migration barrier of 0.2 (0.4) eV, which is a kick-out event. We find the diffusion path between two neighboring *H* sites also to contain the *S* interstitial, from where another BT^0 configuration can be accessed without barrier, or another *H* site can be reached over a barrier of 0.1 (0.1) eV. This suggests an immediately following $B_H^0 \rightarrow BT^0$ step to be the most probable event after the $BT^0 \rightarrow B_H^0$ portion of the diffusion step, which predicts an immediate kick-in event without long-range interstitial diffusion.

For systems with positive charge, we find a one-step process $BT^+ \rightarrow BT^+$ with no intermediate metastable interstitial position, a bond-centered interstitial B_B^+ [Fig. 1(e)] as saddle point, and a migration barrier of 0.8 (1.2) eV. However, there is a second, competing process, especially for the LDA calculations, which has B_H^+ as the saddle point, with a migration barrier of 1.0 (1.3) eV, slightly higher in energy, but with a larger average hopping length and more possible paths.[5] For negatively charged systems, we find a $B_X^- \rightarrow B_S^- \rightarrow B_X^-$ path with an intermediate metastable B_S^- configuration and a migration barrier of 0.6 (0.5) eV. Overall, diffusion and deactivation models derived from these calculations have given excellent results in comparison to experiment.[5,6]

III. BORON DEACTIVATION IN SILICON

The implant-anneal cycle can cause the formation of B precipitates which immobilize and deactivate the B atoms well below the solid solubility limit. From the observation of the trapping of interstitials by these precipitates, it has been concluded that they consist of B–*I* clusters (BICs).

Previously, only one set of BIC reaction barriers from first-principles by the Livermore group for B_nI_m (n<4) clusters had been available,[7] where the influence of the different charge states had been neglected and the structures of the clusters had been guessed under the ad-hoc constraint that all B atoms in BICs are substitutional.[8] However, these numbers could not explain all experiments: In Ref. 9, several of the cluster energies of Ref. 7 had to be refitted in order to predict annealing experiments correctly. Also, the predictions of Ref. 10, based on the cluster energies of Ref. 7, where an "activation window" for B anneals was predicted, have been shown recently not to be in agreement with experiment.[11] However, since Ref. 12, where updated reaction barriers from the Livermore group are given, still reported this activation window, our study was intended to help resolve this important discrepancy between *ab initio* modeling and experiment. In the following, we discuss a systematic study of BIC energetics including the influence of charges and a careful structure minimization within the BIC phase space. The technical details are described in Ref. 6.

We examined a number of BICs B_nI_m with $n,m < 4$, as well as $B_{12}I_7$ (which has been studied theoretically before without presenting formation energy values[13]) and single B atoms in {311} defects. In order to increase our chances to find the global instead of a local minimum, we started for each cluster from many different initial configurations that were structurally relaxed, which, however, does not guarantee that we really found the energetically most favorable structures.

Figure 2 summarizes our first-principles results. For all examined clusters (except for B_4^- and B-{311}) we show the structure, LDA and GGA energies as well as fitted energies from Ref. 14. Displayed are the most stable structures and energies we could find for the lowest-energy charge states at mid. In contrast to tight-binding[15] and inverse modeling[14] results, we find for all substitutional B clusters repulsive energies (0.9, ~2.2, and ~2.5 eV for B_2^-, B_3^{3-}, and B_4^-, respectively), making the existence of such clusters highly improbable. All other clusters have negative formation energy, in contrast to the tight- binding calculations of Ref. 15, which also predict structures different from ours for most of the examined clusters. Calculating reaction barriers from our results, we find in general (especially with GGA) similar numbers to Ref. 12, but also critical differences: Our B_2I_3 cluster is extremely stable against decay with a reaction barrier between 3 and 4 eV; also, our B_3I_2 energy forbids spontaneous decay into a B_3I cluster with a barrier of 1–2 eV. The reason for this discrepancy might be that higher-energy structures and charge states have been considered in Ref. 12, which are less stable than the ones we found in the present work.

We implemented the clustering model from Fig. 2 (excluding $B_{12}I_7^-$ and B-{311}) into a continuum model, combined with our diffusion model for B diffusion and *ab initio* calculated point-defect energetics and prefactors from Ref. 16. For *I* clustering, we mainly use the model from Ref. 17. The results for B activation are shown in Fig. 3. Both LDA and GGA models correctly predict inverse annealing at low temperatures due to the beginning formation of B_3I_2 and B_4I_2. Due to the low energy that we find for B_2I_3, however,

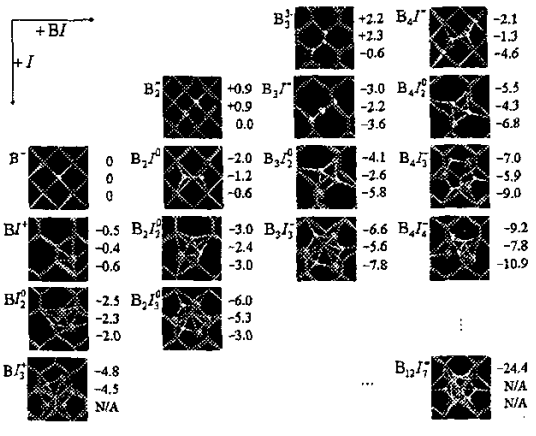

FIG. 2. Structure and energetics of small BICs. Small white balls are B, large gray balls Si atoms involved in the clusters. The energy values (eV) are, top to down, GGA, LDA, and fitted values from Ref. 14.

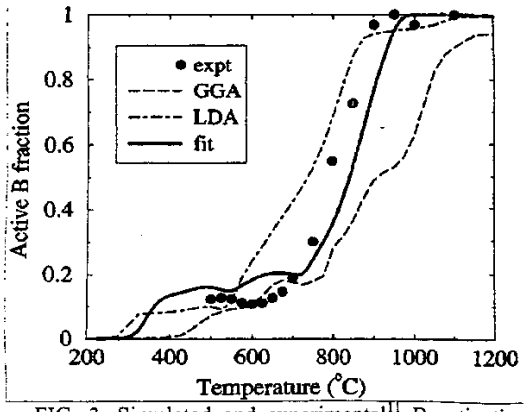

FIG. 3. Simulated and experimental[11] B activation after a 40 keV, 2×10^{14} cm^{-2} B implant for 30 min anneals at varying temperatures. Dashed line: LDA clustering energies; dot-dashed line: GGA energies; solid line: re-fitted to SIMS.

we find in contrast to previous work that also the decay of this high-I content cluster contributes significantly to the activation process at higher temperatures. Thus, it might be desirable to include clusters with higher I content into future work.

LDA predicts too much activation too soon, whereas GGA results in too strong clustering as compared to experiment. In order to improve agreement with experiment, we used a genetic algorithm to refit the parameters to a large number of SIMS data for different annealing conditions. The fit result was mostly independent of the starting parameters and resulted in parameter values which lay with a few exceptions between the LDA and GGA values, which therefore might be considered as upper and lower boundaries for the clustering energies. No activation data were used for the fit. Nevertheless, the experimental data in Fig. 3 are well predicted suggesting that the key physics might be described reasonably well within this model.

IV. MODELING OF DOPANT SEGREGATION

Interfaces between different materials occur frequently in Si processing. Dopants have different solubilities in different materials and thus redistribute at an interface until the chemical potential is the same on both sides of the interface. The flux J across the interface is usually modeled by (e.g., for Si/SiO_2), $J_{Si\to SiO_2} \propto \left(C_{Si} - C_{SiO_2}/k_0\right)$, where C_{Si} and C_{SiO2} are the dopant concentrations on the Si and SiO_2 side, respectively, and the segregation coefficient k_0 is the ratio of the equilibrium doping concentrations on each interface side.[18]

Experimental determination of segregation coefficients between different materials is not trivial: matrix effects on the yield and mixing effects at the interface complicate SIMS profiling of doping concentrations across even thick Si/SiO_2 interfaces. For thin oxides, SIMS does not have adequate resolution. Additionally, especially for B at the Si/SiO_2 interface, the apparent segregation coefficient is strongly influenced by the amount of moisture in the oxidizing ambient. Finally, it is not clear what defines an "equilibrium" dopant concentration in an oxide only a few atomic layers thick and if a steady-state segregation model is valid. Therefore, we examine in the following dopant segregation on an atomic length scale for boron as an example, using first-principles calculations.

The total energy of a boron atom at different locations, which controls the equilibrium dopant concentration, can be used to identify its preferred segregation sites. As our model interface, we use a structure proposed by Buczko *et al.*,[19] which is atomically sharp and has no miscoordination. We find that a semi-periodic, hydrogen-terminated slab geometry gives very similar results to a periodic supercell calculation and report in the following only the latter. Our B diffusion work[5] showed that substitutional B is the ground state for dilute concentrations. Since experiments[20] find that B in SiO_2 prefers as well to substitute Si atom,s we examine in the following an "all-substitutional" $Si_{91}O_{56}B_1$ supercell.

Figure 4 shows the calculated energy of the interface system as a function of the location of the B atom. We find an energy minimum in the last bulk Si layer ~0.4 eV lower than for B in Si far away from the interface [which defines zero energy in Fig. 2(b)], with the energy steeply rising to ~2 eV on the oxide side. Since this results contradicts the experimental findings of B segregating into the oxide[18] this means – provided our interface structure is realistic enough – that crucial other factors which favor the segregation of B into SiO_2 have not yet been considered in our model.

Such an "other factor" could be the presence of point defects. Previous work has suggested that the presence of B in SiO_2 would promote the formation of O vacancies in the oxide, which can be already as high as 10^{18} cm^{-3} in the

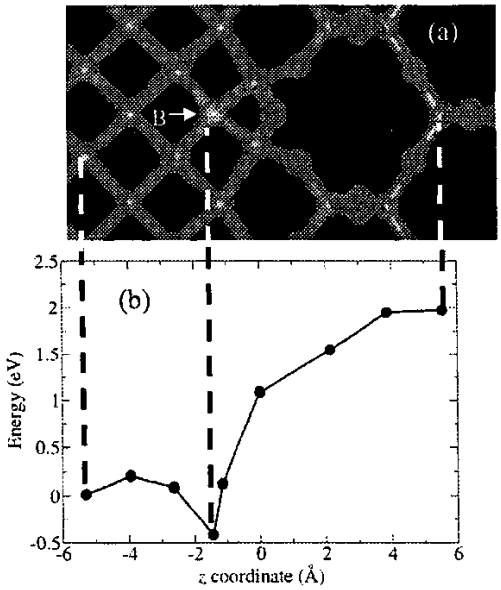

FIG. 4. (a) Examined interface structure with B atom (shown at location of energy minimum). (b) Total energy of supercell as a function of B z coordinate.

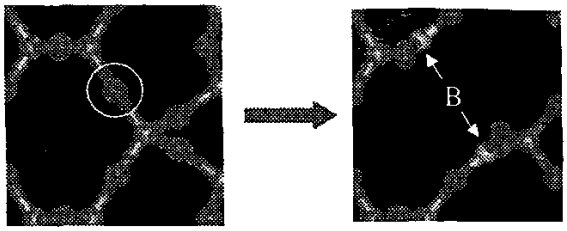

FIG. 5 Creation of two 3-fold coordinated B sites by removing an O atom (circled) from the oxide.

interface region.[20] This would result in a three-fold coordination of B atoms neighboring the O vacancy, a coordination which is found in boron glass, B_2O_3. Indeed, XPS measurements have confirmed the presence of boron glass in SiO_2 doped with ~1% B.[20] Therefore, we examine in the following the segregation energy of a B atom in our interface structure in the presence of an O vacancy in the oxide.

We find in the presence of the O vacancy that the lowest-energy positions for B atoms are the Si sites neighboring the vacancy (Fig. 5). We have studied a system with one vacancy and two B atoms. Once the first B atom is located next to the O vacancy, the second B atom gains 1.5 eV by moving from the Si bulk to the other vacancy-neighboring site and thus would clearly segregate into the oxide. However, we need to mention that this is not the overall lowest-energy structure that we found, since the 2 B atoms in 3rd-neighbor substitutional configuration on the Si side with one of the B atoms in the top Si layer have an energy which is lower by 0.3 eV. Such a 3rd-neighbor configuration has been previously found to have the lowest energy for C in Si.[21]

Although our calculation – which still might be oversimplified, use an unrealistic interface structure, or lack another crucial ingredient – did not find the two B atoms to have the lowest energy on the oxide side, the presence of an O vacancy is clearly shown to promote B segregation into the oxide. Since previous work has suggested a similarly crucial role of point defects for the experimentally observed pile-up of As and P at the Si/SiO_2 interface,[22] we conclude that point defects seem to be necessary in order to explain the observed segregation behavior of dopants.

V. CONCLUSIONS

In this paper, we have shown concepts and examples of physical multiscale process simulation work, which included B diffusion (we find a direct two-step diffusion mechanism), B deactivation (we find in addition to the major features of previous work that pure B clusters without *I*s have forbiddingly high energy and that B_2I_3 should be a third key cluster besides B_3I_2 and B_4I_2), and B interface segregation (we conclude that point defects seem to be necessary in order to explain the observed segregation behavior of dopants). Although much can be learned from *ab-initio* calculations, due to their too-large error bars for defect systems and the large phase space we currently still find it necessary to re-calibrate our final continuum models.

ACKNOLWEDGMENTS

I would like to thank my collaborators on this work, Marius Bunea, Alex Demkov, Scott Dunham, Benjamin Liu, Chun-Li Liu, Mike Masquelier, Roland Stumpf, Blas Uberuaga, and Xiaodong Zhang. Motorola, Inc., is acknowledged for continuing support.

REFERENCES

[1] A. Ural, P. B. Griffin, and J. D. Plummer, J. Appl. Phys. **85**, 6440 (1999).
[2] J. Zhu, T. Diaz de la Rubia, L. H. Yang, C. Mailhiot, and G. H. Gilmer, Phys. Rev. B **54**, 4741 (1996); J. Zhu, Comput. Mater. Sci. **12**, 309.
[3] H. Jónsson, G. Mills, and K. W. Jacobsen, in *Classical and Quantum Dynamics in Condensed Phase Simulations*, edited by B. J. Berne, G. Ciccotti, and D. F. Coker (World Scientific, Singapore, 1998), p. 385.
[4] G. Kresse and J. Hafner, Phys. Rev. B **47**, 558 (1993); **49**, 14 251 (1994); G. Kresse and J. Furthmüller, Comput. Mater. Sci. **6**, 15 (1996); Phys. Rev. B **54**, 11 169 (1996).
[5] W. Windl, M. M. Bunea, R. Stumpf, S. T. Dunham, and M. P. Masquelier, Phys. Rev. Lett. **83**, 4345 (1999).
[6] X.-Y. Liu, W. Windl, and M. P. Masquelier, Appl. Phys. Lett. **77**, 2018 (2000).
[7] J. Zhu (unpublished); partially reported in Ref. 10.
[8] J. Zhu (private communication).
[9] D. Stiebel, P. Pichler, and H. Ryssel, Mater. Res. Soc. Symp. Proc. **538**, 141 (1999).
[10] M. J. Caturla, M. D. Johnson, and T. Diaz de la Rubia, Appl. Phys. Lett. **72**, 2736 (1998).
[11] A. Mokhberi, P. Griffin, and J. D. Plummer (unpublished).
[12] S. K. Theiss, M. J. Caturla, M. D. Johnson, J. Zhu, T. Lenosky, B. Sadigh, and T. Diaz de la Rubia, Thin Solid Films **365**, 219 (2000).
[13] J. Yamauchi, N. Aoki, and I. Mizushima, Phys. Rev. B **55**, 10 245 (1997).
[14] L. Pelaz, G. H. Gilmer, H.-J. Gossmann, C. S. Rafferty, M. Jaraiz, and J. Barbolla, Appl. Phys. Lett. **74**, 3657 (1999).
[15] W. Luo, P. B. Rasband, P. Clancy, and B. W. Roberts, J. Appl. Phys. **84**, 2476 (1998).
[16] B. P. Uberuaga, W. Windl, R. Stumpf, and H. Jónsson (unpublished).
[17] C. S. Rafferty, G. H. Gilmer, M. Jaraiz, D. Eaglesham, and H.-J. Gossmann, Appl. Phys. Lett. **68**, 2395 (1996).
[18] J. D. Plummer, M. D. Deal, and P. B. Griffin, *Silicon VLSI Technology* (Prentice Hall, NJ, 2000), pp. 413.
[19] R. Buczko, S. J. Pennycook, and S. T. Pantelides, Phys. Rev. Lett. **84**, 943 (2000).
[20] M. Mollat, A. A. Demkov, P. Fejes, and D. Werho, J. Vac. Sci. Technol. B **19**, 372 (2001).
[21] M. Meléndez-Lira, J. D. Lorentzen, J. Menéndez, W. Windl, N. G. Cave, R. Liu, J. W. Christiansen, N.D. Theodore and J.J. Candelaria, Phys. Rev. B **56**, 3648 (1997).
[22] J. Dabrowski, R. A. Casali, H.-J. Müssig, R. Baierle, M. J. Caldas, and V. Zavodinsky, J. Vac. Sci. Technol. B **18**, 2160 (2000).